Journal of Engineering Research and Reports

16(2): 10-25, 2020; Article no.JERR.59695
ISSN: 2582-2926

A Study of MHD Casson Fluid Flow over a Permeable Stretching Sheet with Heat and Mass Transfer

K. K. Asogwa[1*] and A. A. Ibe[2]

[1]Department of Mathematics, Nigeria Maritime University, Okerenkoko, Delta State, Nigeria.
[2]Department of Physics, Nigeria Maritime University, Okerenkoko, Delta State, Nigeria.

Authors' contributions

This work was carried out in collaboration with both authors. Author KKA designed the study, performed the mathematical analysis, wrote the protocol and wrote the first draft of the manuscript. Author AAI examined the physics behind the problem. Both authors read and approved the final manuscript.

Article Information

DOI: 10.9734/JERR/2020/v16i217161
Editor(s):
(1) Dr. Hamdy Mohy El-Din Afefy, Tanta University, Egypt.
Reviewers:
(1) R. Vijayakumar, Annamalai University, India.
(2) A. Subba Rao, Madanapalle Institute of Technology & Science, India.
Complete Peer review History: http://www.sdiarticle4.com/review-history/59695

Review Article

Received 29 May 2020
Accepted 05 August 2020
Published 24 August 2020

ABSTRACT

In this paper, we study the numerical approach of MHD Casson fluid flow over a permeable stretching sheet with heat and mass transfer taking into cognizance the various parameters present. A set of suitable local similarity transformations are used to non-dimensionalize the governing equations of the present problem. The system of ordinary differential equations are solved numerically by MATLAB bvp4c solver. The effect of the involved parameters on Velocity, Temperature, and Concentration, Skin friction coefficient, Nusselt number and Sherwood number has been studied and numerical results are presented graphically and in tabular form. The numerical results are in good agreement with those of the results previously published in the literature.

Keywords: Casson fluid; chemical reaction; MHD, radiation; non-newtonian fluid; heat and mass transfer.

**Corresponding author: Email: kanasogwa@yahoo.com, kanasogwa@gmail.com;*

1. INTRODUCTION

The importance of non-Newtonian fluids are found in several branches of engineering applications especially in the extraction of crude oil from petroleum products, such as polymer processing and nuclear fuel debris treatment. Other areas include paper production, manufacturing of food, drugs, flow of blood and flow of plasma. In all cases, non-Newtonian fluids are more appropriate than Newtonian. In order to know the characteristics of non-Newtonian fluid and their applications, it is necessary to study their behavior. Casson fluid model is one kind of non-Newtonian fluid model proposed by Casson [1]. This fluid can be defined as shear thinning fluid example Honey, jelly, and human blood are considered as Casson fluids. This fluid is reduced to Newtonian fluid at a very high shear stress. Magnetohydrodynamic (MHD) is also a non-Newtonian fluid which is a branch of fluid dynamics that deals with the dynamics of electrically conducting fluids. Examples of such fluids include salt water and liquid metals Moreau [2].

Many investigators (Prasad et al. [3] and Rao et al. [4]) had considered modelling laminar transport phenomena in a Casson rheological fluid from a horizontal circular cylinder with partial slip. MHD flow of a Casson fluid due to an impulsively started moving flat plate was considered by Mustafa et al. [5]. Hayat et al. [6] reported Soret and Dufour Effects on magneto hydrodynamic flow of Casson fluid. Pramanik [7], Bhattacharya et al. [8], Bhattaacharyya [9], Mukhopadhyay et al. [10] and Qasim and Noreen [11] had studied related work of Casson fluid flow and heat transfer past an exponentially porous stretching surface in the presence of thermal radiation with different boundary conditions.

Recent advancements in the study of MHD Casson fluid flow, Ramanuja and Nagaradhika [12] investigated MHD analysis of Casson fluid through a vertical porous surface with chemical reaction. Numerical investigation with stability convergence analysis of chemically hydromagnetic Casson fluid flow in the effects of thermophoresis and brownian motion was observed by Mondal et al. [13]. Hasan and Rahman [14] had examined Casson fluid flow and heat transfer over a permeable vertical stretching surface with magnetic field and thermal radiation. Analytical study of Magnetohydrodynamic oscillatory viscoelastic flow with radiation and constant suction over a vertical flat plate in a porous medium was reported by Asogwa et al. [15]. Das et al. ([16] & [17]) investigated hydromagnetic flow of a heat radiating chemically reactive Casson nanofluid past a stretching sheet with convective boundary conditions. Animasaun [18] studied Effects of thermophoresis, variable viscosity and thermal conductivity on free convective heat and mass transfer of non-darcian MHD dissipative Casson fluid flow with suction and nth order of chemical reaction.

Further, researchers, Ibrahim and Makinde [19], Benazir et al. [20] Asogwa [21], Mukhopadhyay [22] and Nadeem et al. [23] had investigated MHD flow of a Casson fluid over an exponentially shrinking sheet. Rizwan et al. [24], Hussain et al. [25] and Kameshwaran et al. [26] had observed Dual solutions of Casson fluid flow over Stretching or Shrinking sheet.

Motivated by the above studies, we have made the endeavor to explore the influence of different physical parameters on the MHD Casson fluid flow over a permeable stretching sheet with heat and mass transfer in the presence of convective boundary conditions in both temperature and concentration with wall velocity. The system has also been incorporated with magnetic field and Casson parameter for both temperature and velocity.

The governing partial differential equations are reduced into the system of ordinary differential equation by using a suitable similarity transformation. Those equations have then been converted into a system of first-order boundary value problem and solved using the MATLAB program bvp4c. The numerical results are compared with the results in the existing literature, and it is found to be in good agreement. The influence of various pertinent parameters of the present model on the flow field, velocity, temperature and concentration has been analyzed through different graphs and tables.

The current study investigates the numerical solutions for a unique class of nonlinear differential equations generated by heat and mass transfer of a permeable stretching sheet is obtained. Casson fluid model is used to classify the non-Newtonian fluid behaviour. Using the similarity transformations, the governing equations have been reduced into a system of ordinary differential equations. These differential equations are nonlinear which cannot be solved

analytically. Hence, MATLAB bvp4c solver has been used for solving it. The flow fields for heat and and mass transfer are significantly affected by the physical parameters.

2. MATHEMATICAL FORMULATION

Consider a steady two dimensional boundary layer MHD flow of a viscous incompressible electrically conducting fluid along a permeable vertical stretching sheet with thermal radiation. Dual equal and opposite forces are introduced along the x-axis so that the sheet is stretched keeping the origin fixed y=0 as shown in Fig. 1. A magnetic field B_0 of uniform strength is applied in y-direction. The effect of the induced magnetic field is not completely neglected in comparison to the applied magnetic field away from the plate. Here x-axis is taken along the direction of the plate and y-axis normal to it.

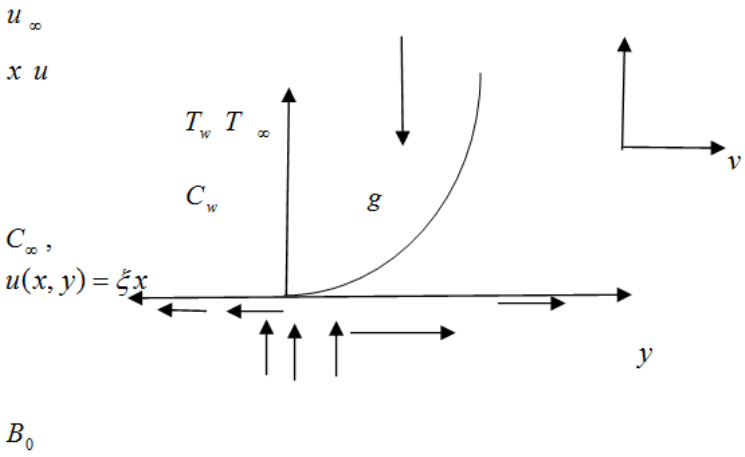

Fig. 1. Schematic diagram of the model

The rheological equation of state for an isotropic and incompressible flow of a Casson fluid is as follows.

$$T_{ij} = \begin{cases} \left(\mu_B + \frac{p_y}{\sqrt{2\pi}}\right) 2e_{ij} & \pi > \pi_c \\ \left(\mu_B + \frac{p_y}{\sqrt{2\pi}}\right) 2e_{ij} & \pi < \pi_c \end{cases} \tag{1}$$

Where μ_B is the plastic dynamic viscosity of non-Newtonian fluid, and p_y is the yield stress of the fluid, $\pi = e_{ij}e_{ij}$ and e_{ij} are the $(i,j)^{th}$ component of the deformation, π is the product of the component of deformation rate with itself, π_c is the critical value of π based on non- Newtonian model. The governing equations for the steady boundary layer flow of non-Newtonian Casson fluid can be written as follows

$$u_x + v_y = 0 \tag{2}$$

$$uu_x + vu_y = \nu\left(1 + \frac{1}{\beta}\right)\left(u_{yy}\right) + g\beta_1\left(T - T_\infty\right) + g\beta_2\left(C - C_\infty\right) - \frac{\sigma B_0^2}{\rho}\left(u - U_\infty\right) \tag{3}$$

$$uT_x + vT_y = \alpha\left(T_{yy}\right) + \frac{\nu}{\rho C_p}\left(1+\frac{1}{\beta}\right)\left(u_{yy}\right) + \frac{\sigma B_0^2}{\rho}\left(u-U_\infty\right)^2 - \frac{1}{\rho C_p}\left(\frac{\partial q_r}{\partial y}\right) \tag{4}$$

$$uC_x + vC_y = D\left(C_{yy}\right) - K_c\left(C - C_\infty\right) \tag{5}$$

With the following boundary conditions:

$$\left.\begin{aligned} &u = \xi x,\ v = v_w,\ T = T_\omega,\ C = C_\omega,\ at\ \ y = 0 \\ &u \to 0, \qquad T \to T_\infty,\ C \to C_\infty,\ as\ \ y \to \infty \end{aligned}\right\} \tag{6}$$

Where u and v are the velocity components in the x and y directions, ν is the kinematics viscosity, ξx is the assumed wall velocity and v_w is the Suction velocity, K_c is the chemical reaction term, T is the fluid temperature, C is the mass concentration, g is the gravitational constant, β_1 and β_2 are the thermal expansions of fluid and concentration, $\beta = \mu_B\left(\frac{2\pi_c}{P_y}\right)$ is the Casson fluid parameter, ρ is the fluid density, C_p is the specific heat capacity, k is the thermal conductivity, D is the diffusion term, B_0 is the magnetic field and q_r is the radiative heat flux.

Assuming the Rosseland approximation is

$$q_r = -\frac{4\sigma^*}{3k^*}\frac{\partial T^4}{\partial y} \tag{7}$$

σ^* is the Stefan Boltzmann, k^* is the mean absorption effect for thermal radiation constant. We assume that the temperature differences within the flow are sufficiently small such that T^4 can be expanded in a Taylor series about T_∞ and neglecting higher order terms gives

$$T^4 = 4TT_\infty^3 - 3T_\infty^4 \tag{8}$$

Hence (7) becomes

$$\frac{\partial q_r}{\partial y} = \frac{16\sigma^* T_\infty^3 (T - T_\infty)}{3k^*} \tag{9}$$

Substituting (9) into (4) gives

$$uT_x + vT_y = \alpha\left(T_{yy}\right) + \frac{\nu}{\rho C_p}\left(1+\frac{1}{\beta}\right)\left(u_{yy}\right)^2 + \frac{\sigma B_0^2}{\rho}\left(u-U_\infty\right)^2 - \frac{16\sigma^* T_\infty^3 (T - T_\infty)}{3k^* \rho C_p} \tag{10}$$

The similarity variables are

$$\eta = y\sqrt{\frac{\xi}{\nu}},\ \psi = \sqrt{\xi\nu}xf(\eta),\ \theta(\eta) = \frac{T - T_\infty}{T_\omega - T_\infty},\ \ \phi(\eta) = \frac{C - C_\infty}{C_\omega - C_\infty} \tag{11}$$

Where ψ is the stream function defined as $u = \frac{\partial \psi}{\partial y}$ and $v = -\frac{\partial \psi}{\partial x}$ which satisfies the continuity equation (2). By using this definition, we obtain:

$$u = \xi v x f'(\eta), \quad v = -\sqrt{\xi v} f(\eta) \tag{12}$$

Substituting equations (11) and (12) into equations (3), (5), (6) and (10) above, the transformed equations become:

$$\left(1+\frac{1}{\beta}\right) f_{\eta\eta\eta} + f f_{\eta\eta} - M\left(f_\eta - 1\right) - (f_\eta)^2 + Gr\theta + Gr\phi = 0 \tag{13}$$

$$\frac{1}{\Pr}\left(1+\frac{4}{3}R\right)\theta_{\eta\eta} + f\theta_\eta + Ec\left(1+\frac{1}{\beta}\right)\left(f_{\eta\eta}\right)^2 + Ec\left(f_\eta - 1\right)^2 M = 0 \tag{14}$$

$$\phi_{\eta\eta} + Sc\, f\phi_\eta - ScK\phi = 0 \tag{15}$$

The corresponding boundary condition

$$\left.\begin{array}{l} f_\eta(0) = 1, \quad f(0) = f_w, \quad \theta(0) = 1, \ \phi(0) = 1, \ at \ \ \eta = 0 \\ f(\infty) \to 0, \qquad \theta(\infty) = 0, \ \phi(\infty) = 0, \ as \ \ \eta \to \infty \end{array}\right\} \tag{16}$$

Where $M = \frac{\sigma B_0^2}{\rho \xi}$, $R = \frac{4\sigma^* T_\infty^3}{k k^*}$, $Gr = \frac{g\beta_1\left(T_\omega - T_\infty\right)}{\xi u}$, $Gc = \frac{g\beta_2\left(C_\omega - C_\infty\right)}{\xi u}$,

$$Ec = \frac{u^2}{C_P\left(T_\omega - T_\infty\right)}, \quad Sc = \frac{v}{D}, \quad K = \frac{K_c}{\xi}, \quad \Pr = \frac{\mu c_\rho}{\kappa}, \quad f_w = -\frac{v_w}{\sqrt{\xi v}}$$

3. SKIN FRICTION, HEAT, AND MASS TRANSFER COEFFICIENTS

The local skin friction coefficient, and rate of heat and mass transfer, respectively, are

$$\mathrm{Re}_x^{\frac{1}{2}} C_f = \left(1+\frac{1}{\beta}\right) f''(0), \ Nu_x \,\mathrm{Re}_x^{-\frac{1}{2}} = -\theta'(0), \ Sh_x \,\mathrm{Re}_x^{-\frac{1}{2}} = -\phi'(0) \tag{17}$$

4. METHODOLOGY

4.1 Numerical Solution Using Collocation Method

The first order differential equations are obtained from equations (13) to (15) using the following relations: Let $f = x_1$, $f_\eta = x_2$, $f_{\eta\eta} = x_3$, $\theta = x_4$, $\theta_\eta = x_5$, $\phi = x_6$, $\phi_\eta = x_7$.

Hence, the following system is generated

$$x_1' = x_2$$

$$x_2' = x_3$$

$$x_3' = \frac{-x_1 x_3 + M\left(x_2 - 1\right) + (x_2)^2 - Gr\theta - Gr_C\phi}{\left(1 + \frac{1}{\beta}\right)}$$

$$x_4' = x_5$$

$$x_5' = \frac{-\Pr x_1 x_5 - \Pr Ec\left(1 + \beta^{-1}\right)\left(x_3\right)^2 - \Pr Ec(x_2 - 1)^2 M}{\left(1 + \frac{4}{3}R\right)}$$

$$x_6' = x_7$$

$$x_7' = -Sc\, x_1 x_7 - ScKx_6$$

The above system is solved using a MATLAB boundary valued problem solver called **bvp4c**. This inbuilt program solves boundary value problems for differential equations of the form

$x' = f\left(x^*\ y\ p\right)$, $\left[a\ \ b\right]$ by implementing a collocation method subject to general nonlinear, two point boundary conditions g(x(a), x(b), p). Where p is a vector of unknown parameters Shampine and Kierzenka [27].

5. RESULTS AND DISCUSSION

Using the inbuilt bvp4c embedded on MATLAB software package, the solutions are obtained for the velocity, temperature and concentration fields respectively, taking into cognizance the effects of the parameters present namely; Radiation effect, Casson parameter, Thermal grashof number, Mass grashof number, Chemical reaction, Hartmann number, Suction parameter, Eckert number, Prandtl and Schmidt numbers. The solutions of the model have been presented in graphs and tables. The effects of various parameters have been depicted in Figs. 2–17, whereas the shear stress, Nusselt number, and rate of mass transfer have been computed and presented in Table 2. The present study is also compared (Table 1) with the available results of Das et al. [16] and found to be in good agreement.

In this study, the fixed values of the governing parameters are taken as $\beta = 0.5$, M = 1.0,

Pr = 0.71, Gr =Gc =3, Sc = 0.3, K = 0.3, η = 1.0, fw = 0.5, K =0.5, Ec=0.1

From Fig. 2. It is observed that the fluid velocity decreases with increasing values of the magnetic parameter M. An opposite force is developed in the direction of the fluid flow due to the presence of magnetic field, which is called the Lorentz force. The Lorentz force has a tendency to reduce the momentum boundary layer thickness. Hence, Lorentz force provides resistance to flow.

Fig. 3. Temperature increases with increase in the magnetic field strength M which implies that under the action of a magnetic field in an electrically conducting fluid a resistive force is developed which causes reduction of flow and an enhancement of temperature.

Fig. 4. It is observed that the velocity increases with an increase in the values of Casson parameter. It is important to note that an increase in Casson parameter makes the velocity boundary layer thickness shorter. It is further observed from this graph that when the Casson parameter is large enough, the non-Newtonian behaviors disappear, and the fluid purely behaves like a Newtonian fluid. Thus, the velocity boundary layer thickness for Casson fluid is larger than the Newtonian fluid. It occurs

because of plasticity of Casson fluid, when Casson parameter decreases the plasticity of the fluid increases, which causes the increment in velocity boundary layer thickness.

Fig. 5. It is observed that the fluid temperature is enhanced with a rise in Casson parameter and Joule heating within the wall of the plate. This may be attributed to additional internal heat generated within the fluid due to flow resistance caused by Lorenz force in the magnetic field.

The nature of Prandlt number Pr on dimensionless velocity and temperature profiles have been displayed in the Figs. 6 and 7. The velocity and temperature profiles decrease when the values of Pr increases. Prandtl number signifies the ratio of momentum diffusivity to thermal diffusivity. This implies that fluids with lower Pr have higher thermal conductivity. So heat can defuse from the sheet faster than for higher Prandtl number fluids.

Figs. 8 and 9 display the effect of Schmidt number (Sc) on the velocity and concentration profiles. It is noticed that the values of Schmidt number increases with decreasing flow of the velocity and concentration profiles. This validates that the heavier diffusing species have a greater retarding effect on the velocity and concentration profiles of the flow field.

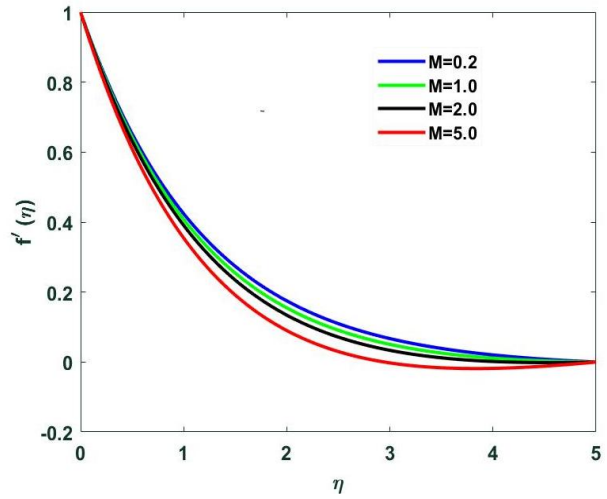

Fig. 2. Variation of M on velocity profiles

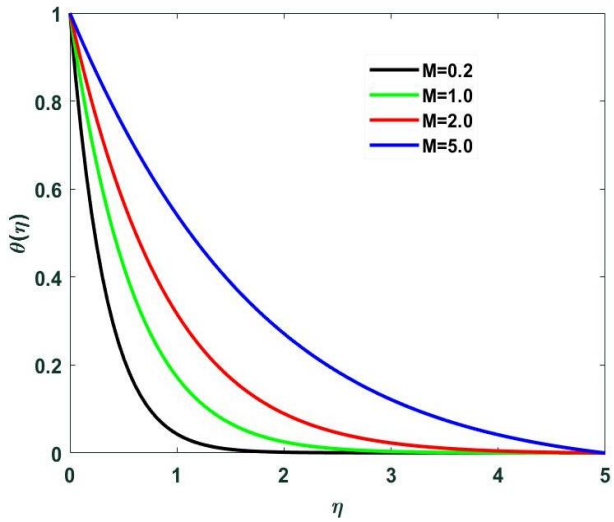

Fig. 3. Variation of M on temperature profiles

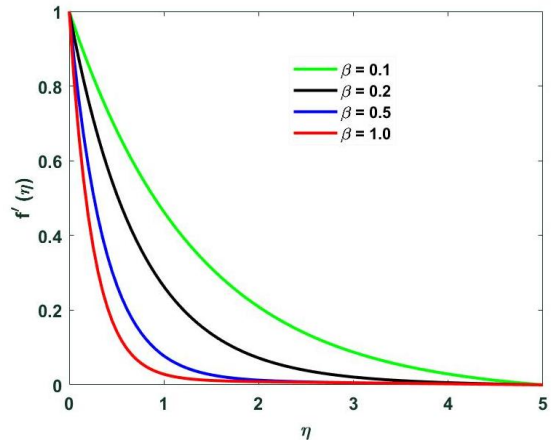

Fig. 4. Variation of β on velocity profiles

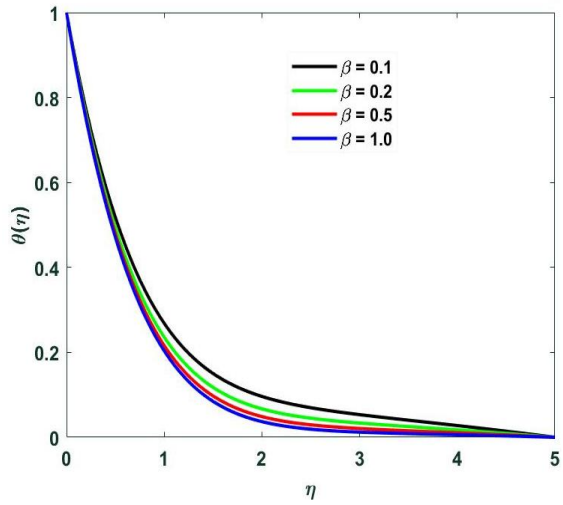

Fig. 5. Variation of β on temperature profiles

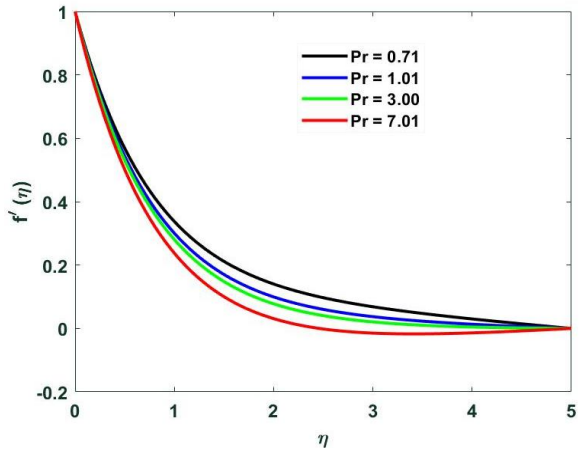

Fig. 6. Variation of Pr on velocity profiles

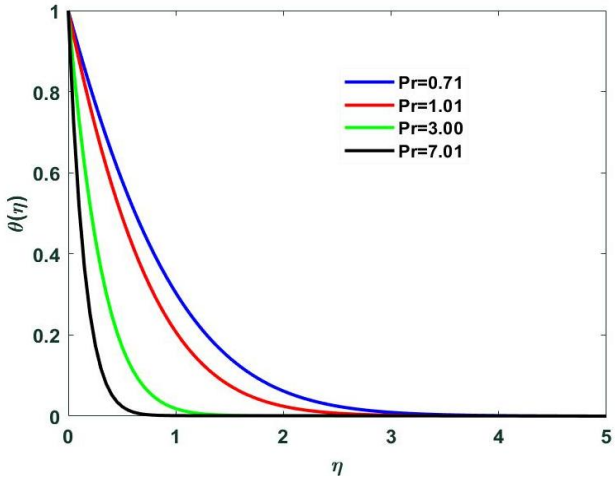

Fig. 7. Variation of Pr on temperature profiles

Fig. 10 Shows the disparity of the velocity profile for various values of the thermal grashof number. It is found from this figure that the velocity profile increases by increasing the values of Gr. The Grashof number signifies the relative effect of the thermal buoyancy force to the viscous hydrodynamic force in the boundary layer. It is seen that there is a rise in the velocity due to the enhancement of thermal buoyancy force.

Fig. 11 Shows the variation of the velocity profile for various values of the mass grashof number. It is seen from this figure that the velocity profile increases by increasing values of Gc. An increase in Grashof number Gc for mass transfer increases the skin friction and declines the rate of heat transfer. Gc is the ratio of the species buoyancy force to the viscous hydrodynamic force.

The behavior of suction parameter fw on velocity, temperature and concentration profiles can be found in Figs. 12, 13 and 14. It is observed that when wall suction is increased, this causes a decrease in the boundary layer thickness and the velocity field is reduced. Again temperature and concentration fields decreases with increasing suction. The temperature and concentration fields become much more suppressed because of increased suction. So, this parameter has dominating effects on velocity, temperature and concentration profiles.

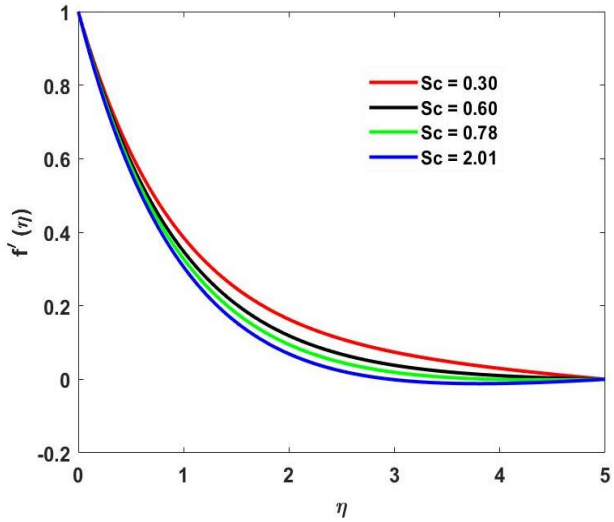

Fig. 8. Variation of Sc on velocity profiles

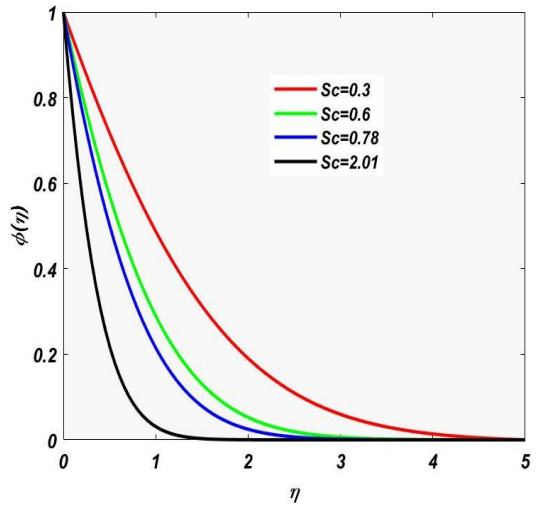

Fig. 9. Variation of Sc on concentration profiles

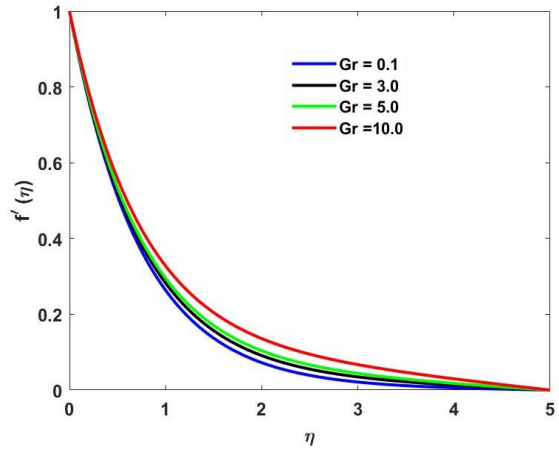

Fig. 10. Variation of Gr on velocity profiles

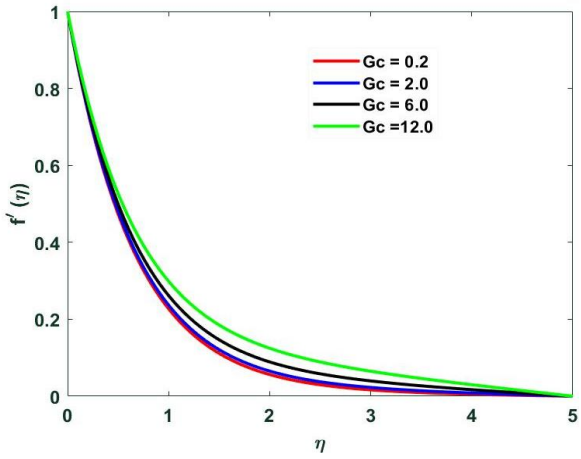

Fig. 11. Variation of Gc on velocity profiles

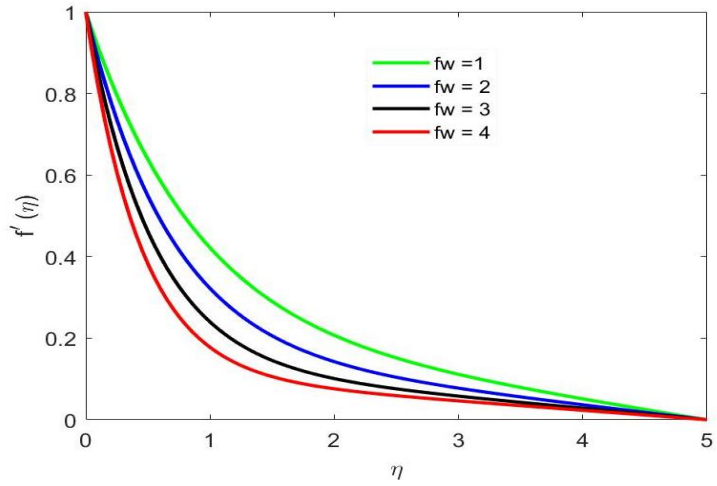

Fig. 12. Variation of fw on velocity profiles

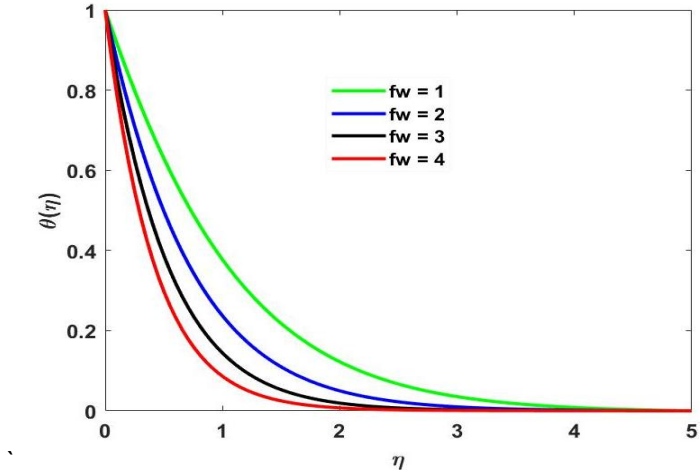

Fig. 13. Variation of fw on temperature profiles

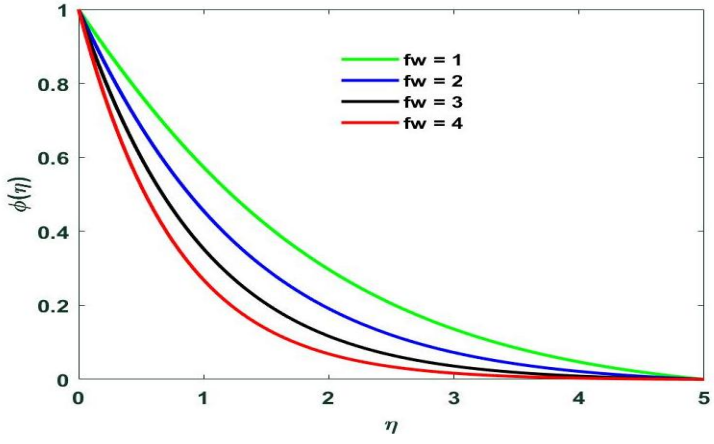

Fig. 14. Variation of fw on concentration profiles

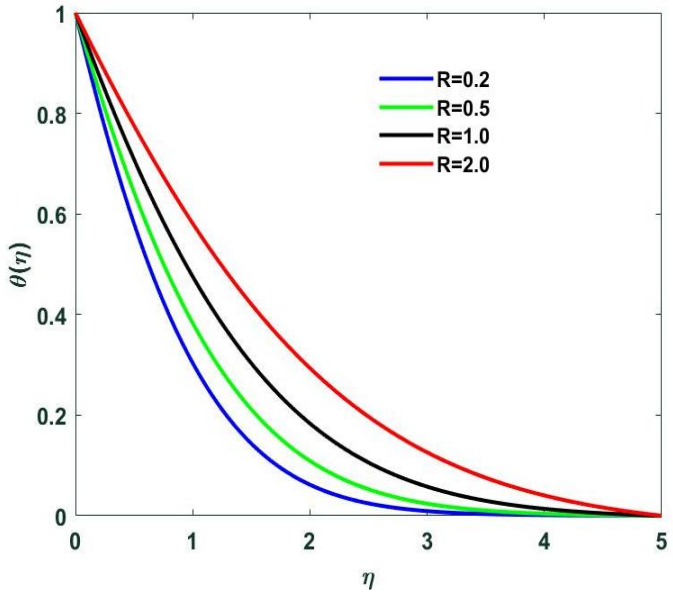

Fig. 15. Variation of R on temperature profiles

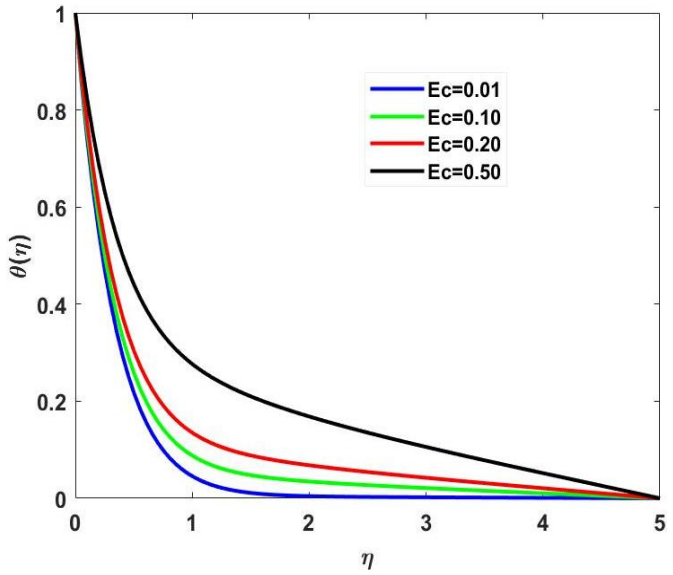

Fig. 16. Variation of Ec on temperature profiles

Table 1. Comparison of skin friction coefficient of the present model with the results in the literature of Das *et al.* [16], Pr=0.71, Sc=0.3, Gr=Gc=3, $\beta = 0.5$, M=1.0, fw = 0.5

Pr	Sc	Gr	β	Das et al. [16]	Present result
0.3	0.3	3	0.5	1.029919	1.029901
0.71	0.6	3	0.5	1.291663	1.291654
0.3	0.3	3	0.5	0.856995	0.855768
0.3	0.78	5	0.5	0.939520	0.939727
0.3	2.01	3	1	-	1.130220

Table 2. Numerical values of skin friction, nusselt number, and sherwood number for various parameters governing the model

M	K	R	Sc	Pr	Ec	fw	Gr	Gc	β	$\left(1+\frac{1}{\beta}\right)f''(0)$	$-\theta'(0)$	$-\phi'(0)$
1.0	0.1	0.1	0.3	0.7	0.2	0.5	2.0	2.0	0.5	1.111236	0.1115	0.1005
1.0	0.1	0.1	0.3	0.7	0.3	1.0	2.0	2.0	0.5	1.121004	0.2225	0.1201
1.5	0.5	0.1	0.3	0.7	0.2	1.0	3.0	2.0	0.5	1.123600	0.2996	0.1220
1.5	0.1	0.1	0.3	1.0	0.3	1.0	3.0	2.0	0.5	1.125568	0.1220	0.1350
1.5	0.2	0.1	0.3	1.0	0.2	1.0	3.0	2.0	0.5	1.150004	0.1350	0.1435
1.5	0.1	0.1	0.3	0.7	0.2	2.0	3.0	2.0	0.5	1.261704	0.2225	0.1466
1.5	0.1	0.2	0.3	0.7	0.2	2.0	3.0	2.0	0.5	1.291658	0.2335	0.1498
2.0	0.1	0.2	0.3	0.7	0.2	2.0	3.0	2.0	0.5	1.298855	0.2996	0.1591
3.0	0.2	0.2	0.3	0.7	0.2	2.0	3.0	2.0	0.5	1.355500	0.3220	0.1600
1.0	0.3	0.2	2.0	1.0	0.2	3.0	3.0	2.0	0.5	1.445453	0.4550	0.1015
2.0	0.5	0.2	0.3	1.0	0.2	3.0	3.0	2.0	0.5	1.879780	0.4568	0.1759
2.0	0.5	0.2	0.3	3.0	0.2	1.0	3.0	2.0	3.0	1.100444	0.6070	0.1811
2.0	0.5	0.2	0.3	3.0	0.2	1.0	3.0	2.0	5.0	1.000524	0.6775	0.1842
3.0	0.6	0.2	0.3	3.0	0.2	2.0	3.0	2.0	5.0	1.004561	0.9898	0.1802
0.5	0.5	0.2	0.6	7.0	0.2	2.0	3.0	2.0	5.0	2.451604	1.00298	0.2055
0.5	2.0	0.3	0.6	7.0	0.2	2.0	3.0	2.0	5.0	2.516337	1.00770	0.26759

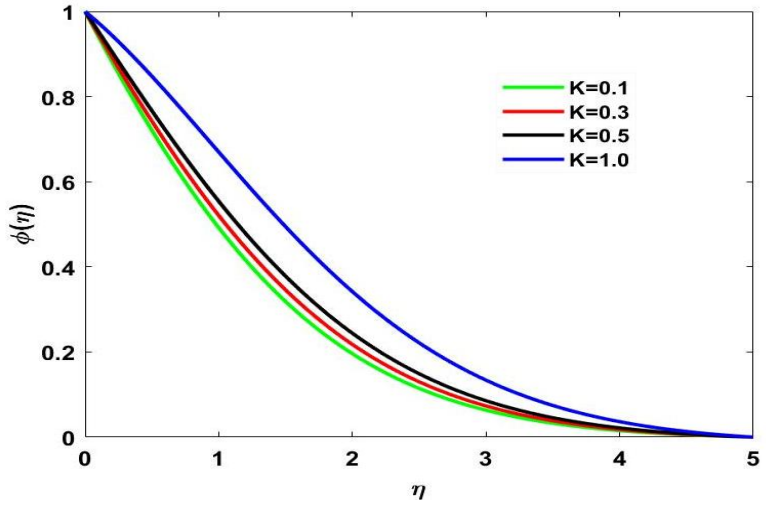

Fig. 17. Variation of K on concentration profiles

Fig. 15 Depicts the temperature profile for various values of radiation (R). It is found from this figure that the temperature profile increases by increasing values of R. The radiation parameter R defines the relative contribution of conduction heat transfer to thermal radiation transfer. It is obvious that an increase in the radiation parameter results to an increasing temperature within the boundary layer.

Fig. 16 Temperature profile for various values of Eckert number (Ec). It is found from this figure that the temperature profile increases by increasing values of Ec.

Fig. 17 Depicts the disparity of the concentration profile for various values of the reactive parameter (K). It is observed from this figure that the concentration profile decreases by increasing the values of K. It is also observed that a destructive reaction greater than zero reduces the concentration profile.

6. CONCLUSION

In this research article, a study of MHD Casson fluid flow over a permeable stretching sheet with heat and mass transfer has been investigated. Some of the significant points of the present work are listed as below:

1. Velocity profile decreases with increasing values of β, M, Pr, Sc and fw while Gr and Gc increases with increasing values.
2. The fluid temperature and concentration profiles reduces with increasing values of Pr, K and Sc respectively.
3. Heat and mass transfer rate are not highly significant with the Casson number.
4. Nusselt number and Sherwood number display an increasing nature with growing values of magnetic parameter.
5. An increase in the values of Sc enhances the skin friction and the heat transfer rate near the plate, while an increase in the values of Pr, heat transfer rate is reduced
6. The skin friction decreases with increase in β.
7. When K increases, the shear stress and the heat transfer rate near the plate get enhanced but reverse trend is being observed in case of mass transfer rate with increasing values of M.

COMPETING INTERESTS

Authors have declared that no competing interests exist.

REFERENCES

1. Casson N. A flow equation for pigment oil-suspensions of the printing ink type, In: Mill CC, editor. Rheology of disperse systems. Pergamon Press. 1959;84.
2. Moreau R. “Magnentohydrodynamics”. Kluwer Academic Publishers; 1990.
3. Ramachandra Prasad V, Subba Rao A, Bhaskar Reddy N. Modelling Laminar Transport Phenomena in a Casson rheological fluid from a Horizontal Circular Cylinder with Partial Slip, I. Mech E. Journal of Process Engineering. 2013;227: 309-326,2013.

4. Subba Rao A, Ramachandra Prasad V, Harshavalli K, Osman Anwar Beg. Thermal radiation effects on non-newtonian fluid in variable porosity regime with partial slip. Journal of Porous Media. 2016;313-329.
5. Mustafa M, Hayat T, Pop I, Aziz A. Unsteady boundary layer flow of a Casson fluid due to an impulsively started moving flat plate, Heat Transfer-Asian Research. 2011;40(6):563-576.
6. Hayat T, Shehzad SA, Alsaedi A, Soret, Dufour. Effects on magneto hydrodynamic flow of Casson fluid, Appl. Math. Mech. 2012;33:301-1312.
7. Pramanik S. Casson fluid flow and heat transfer past an exponentially porous stretching surface in presence of thermal radiation, Ain Shams Engg. J; 2013. (Aricle in Press)
8. Bhattacharya K, Vajravelu K, Hayat T. Slip effect on parametric space and the solution for the boundary layer flow of Casson fluid over a non-porous stretching/shrinking sheet. Int. J. Fluid Mech. Research. 2013; 40:482-493.
9. Bhattaacharyya K. MHD stagnation point flow of Casson fluid and heat transfer over stretching sheet with thermal radiation. Journal of Thermodynamics; 2013. DOI.org/10.1155/2013/169674
10. Mukhopadhyay S, Ranjan De P, Bhattacharyya K, Layek GC. Casson fluid flow over an unsteady stretching surface. , Ain. Shams. Engineering Journal. 2013;4: 933-938.
11. Qasim M, Noreen S. Heat transfer in the boundary layer flow of a Casson fluid over a permeable shrinking sheet with viscous dissipation, Eur. Phys. J. Plus. 2014;7:129.
12. Ramanuja M, Nagaradhika V. MHD analysis of casson fluid through a vertical porous surface with chemical reaction. Global Scientific Journals. 2020;8(4). ISSN 2320-9186
13. Mondal M, Biswas R, Shanchia K, Hassan M, Ahmed SF. Numerical investigation with stability convergence analysis of chemically hydromagnetic casson fluid flow in the effects of thermophoresis and brownian motion. International Journal of Heat and Technology. 2019;3:59-70.
14. Hasan MM, Zillur Rahman. Casson fluid flow and heat transfer over a permeable vertical stretching surface with magnetic field and thermal radiation. IOSR Journal of Engineering. 2019;09(1:14-19. ISSN (e): 2250-3021, ISSN (p): 2278-8719.
15. Asogwa KK, Ibe AA, Udo UM. Magnetohydrodynamic oscillatory viscoelastic flow with radiation and constant suction over a vertical flat plate in a porous medium. IOSR Journal of Mathematics. 2019;15(6):20-30.
16. Das M, Mahanta G, Shaw S, Parida SB. Unsteady MHD chemically reactive double-diffusive casson fluid past a flat plate inporous medium with heat and mass transfer, Heat Transfer- Asian Res. 2019; 1761-1777 wiley periodicals.
17. Das M, Mahanta G, Parida SB, Nandkeolyar R. Hydromagnetic flow of a heat radiating chemically reactive Casson nanofluid past a stretching sheet with convective boundary conditions. In: R. Sharma (Ed.), AIP Conference Proceedings. Vol. 1975, No. 1. Himachal Pradesh: AIP Publishing. 2018;030015.
18. Animasaun IL. Effects of thermophoresis, variable viscosity and thermal conductivity on free convective heat and mass transfer of non-Darcian MHD dissipative Casson fluid flow with suction and nth order of chemical reaction. J Niger Math Soc. 2015; 34(1):11-31.
19. Ibrahim W, Makinde OD. Magnetohydrodynamic stagnation point flow and heat transfer of Casson nanofluid past a stretching sheet with slip and convective boundary condition. Journal of Aerospace Engineering. 2016;29(2). Article# 04015037
20. Benazir AJ, Sivaraj R, Makinde OD. Unsteady magnetohydrodynamic Casson fluid flow over a vertical cone and flat plate with non-uniform heat source/sink. International Journal of Engineering Research in Africa. 2016;21:69-83.
21. Asogwa KK. Numerical solution of hydromagnetic flow past an infinite vertical porous plate. Transactions of the Nigerian Association of Mathematical Physics. 2017;4:143–150.
22. Swati Mukhopadhyay. Casson fluid flow and heat transfer over a nonlinearly stretching surface, Chin. Phys. B. 2013; 22(7):1-6.
23. Nadeem S, Rizwan UH, Lee C. MHD flow of a Casson fluid over an exponentially shrinking sheet, Scientia Iranica B. 2012; 19:1550-1553.
24. Rizwan Ul Haq S, Nadeem ZH, Khan TG Okedayo. Convective Heat transfer and

MHD effects On Casson nano fluid over a shrinking sheet cent. Eur. J. Phys. 2014;12(12):862-871.

25. Hussain T, Shehzeb SA, Alsaedi A, Hayat T, Ramzon M. Flow of Casson Nano fluid with viscous dissipation and convective conditions. A mathematical model J Cent. South Uni. 2015;22:1132-1140.

26. Kameshwaran PK, Shaw S, Sibanda P. Dual solutions of Casson fluid flow over Stretching or Shrinking sheet. Sadhana. 2014;39(6):1573-1583.

27. Kierzenka J, Shampine LF. A BVP solver based on residual control and the MATLAB PSE. ACM Toms. 2001;27(3): 299–316.

Peer-review history:
The peer review history for this paper can be accessed here:
http://www.sdiarticle4.com/review-history/59695